

PAPER • OPEN ACCESS

Coarsening in the long-range Ising model: Metropolis versus Glauber criterion

To cite this article: Wolfhard Janke *et al* 2019 *J. Phys.: Conf. Ser.* **1163** 012002

View the [article online](#) for updates and enhancements.



IOP | ebooks™

Bringing you innovative digital publishing with leading voices to create your essential collection of books in STEM research.

Start exploring the collection - download the first chapter of every title for free.

Coarsening in the long-range Ising model: Metropolis versus Glauber criterion

Wolfhard Janke, Henrik Christiansen and Suman Majumder

Institut für Theoretische Physik, Universität Leipzig, Postfach 100 920, 04009 Leipzig,
Germany

E-mail:

wolfhard.janke@itp.uni-leipzig.de

henrik.christiansen@itp.uni-leipzig.de

suman.majumder@itp.uni-leipzig.de

Abstract. Coarsening kinetics of systems with long-range interactions has, for a long time, only been attempted by truncating the potential using a cut-off distance. In such simulations of the long-range Ising model, one finds effectively short-range like behavior. This contradicts a longstanding theoretical prediction for the growth of the characteristic length scale for this model. We recently performed simulations of this system without the use of a cut-off and, for the first time, confirmed the analytic prediction numerically. Here, we investigate the properties of the used algorithm in more detail and present a comparison of coarsening using the Metropolis and the Glauber criteria.

1. Introduction

Coarsening is a very general phenomenon occurring in many physical situations. At high temperature, systems are generally in a disordered state with high symmetry (e.g., paramagnetic), whereas at low temperature the symmetries are broken and the system is in an ordered state (e.g., ferromagnetic). When one now subjects such a disordered system to external conditions that would correspond to an ordered state, one can observe the growth of ordered regions or domains with time t . The purpose of coarsening analysis is to quantify this nonequilibrium process. This is usually done by calculating a characteristic length scale $\ell(t)$, which quantifies the size of the ordered structures. For the short-range interacting Ising model with non-conserved order parameter, the growth follows the Lifshitz-Cahn-Allen law $\ell(t) \sim t^{1/2}$ [1, 2]. There exist several simulation studies which numerically confirm this prediction for the short-range Ising model [3, 4]. Long-range interactions are omnipresent in nature and other sciences, ranging from electrostatic forces over neuroscience to economical phenomena [5, 6, 7, 8, 9]. Thus to correctly describe such physical systems, one needs to take those long-range interactions into account. Here, we study the long-range interacting Ising model with Hamiltonian

$$\mathcal{H} = - \sum_i \sum_{i < j} J(r_{ij}) s_i s_j, \quad (1)$$



where $s_i = \pm 1$ are spins and the long-range interactions are chosen to decay algebraically with

$$J(r_{ij}) = \frac{1}{r_{ij}^{d+\sigma}}. \quad (2)$$

Here $r_{ij} = |\vec{r}_{ij}| = |\vec{r}_i - \vec{r}_j|$ is the distance between two spins and d is the dimension of the system. How long-range the potential is can be tuned by σ , where $\sigma = \infty$ corresponds to the short-range Ising model. Note, that the summation is performed over the whole lattice, i.e., every spin interacts with every other spin. For this model, there exists a prediction for the growth of $\ell(t)$ in dependence of σ , given by [10, 11, 12]

$$\ell(t) = \begin{cases} t^{1/2} & \sigma > 1 \\ [t \log(t)]^{1/2} & \sigma = 1, \\ t^{1/(1+\sigma)} & \sigma < 1 \end{cases}, \quad (3)$$

implying that the short-range scaling behavior already sets in for $\sigma > 1$. Here, the crossover value $\sigma_{\times} = 1$ is expected to be dimension independent. This is in contrast to the crossover values σ_{\times} in equilibrium, which are still disputed and dependent on the spatial dimension [13, 14, 15, 16, 17, 18]. There have been previous numerical studies using Monte Carlo simulations for the coarsening in the long-range Ising model, in which a cut-off of the potential was used to make the simulation tractable [19, 9]. Ref. [9] reported that the coarsening dynamics was effectively short-range, i.e., $\ell(t) \sim t^{1/2}$ for all σ .

The treatment of the full range of long-range interactions in simulations often leads to problems that are no longer computationally tractable. In some cases, e.g., the long-range interacting Ising model, there exist specialized cluster algorithms based on the Swendsen-Wang algorithm [20] that enable efficient simulations of such systems [21, 22, 23]. However, those algorithms are only meaningful in equilibrium simulations where one is interested in sampling the equilibrium distribution, i.e., the moves do not need to have a physical equivalence. However, when studying dynamics, one requires a physical evolution in time and thus is restricted to single spin or particle dynamics. We recently performed simulations by utilizing the trick of storing the effective field for each spin.¹ With this method, when applied to the coarsening of the two-dimensional Ising model, we obtained a significant speedup by a factor of the order of 1000 [25]. Regarding the coarsening dynamics, we were able to confirm, for the first time, the above mentioned long-standing analytical prediction (3) [10, 11, 12]. In this work, we will present some further details of the method as well as the algorithm and additionally compare Metropolis and Glauber update dynamics. We end with a detailed analysis of the growth exponent by performing a finite-size scaling analysis.

2. Model, Method, and Algorithm

2.1. Algorithm

In usual canonical, i.e., fixed temperature, Monte Carlo simulations of the short-range Ising model with Hamiltonian

$$\mathcal{H} = -J \sum_{\langle ij \rangle} s_i s_j, \quad (4)$$

one calculates the change in energy ΔE by considering the local energy change by essentially summing over the nearest neighbors. This is done at every spin-flip attempt. The spin flip is then most commonly accepted by the Metropolis criterion [26] for a flip of spin s_i ,

$$p_M(s_i) = \min[1, \exp(-\Delta E_i/T)]. \quad (5)$$

¹ We thank Alfred Hucht for pointing out to us at this conference, that such a method has already been briefly mentioned in Ref. [24] dealing with simulations of the Heisenberg model with dipole interactions.

Generally, and also in our simulation, all physical constants, such as the Boltzmann constant k_B , are set to unity. Alternatively, one could also use the acceptance criterion of Glauber [27],

$$p_G(s_i) = 0.5[1 - \tanh(0.5\Delta E_i/T)], \quad (6)$$

which is considered to be more physical. Both p_M and p_G fulfill the criterion of detailed balance in equilibrium. In an equilibrium simulation the Glauber update generally possesses a smaller autocorrelation time. For the long-range interacting Ising model, the calculation of ΔE is computationally much more demanding, as not only the nearest neighbors but also all other spins have to be considered. Thus one tries to limit the number of times one has to calculate this sum. The idea of storing the effective field for each spin arises from the very trivial observation, that during a single Monte Carlo sweep typically never all spins flip (unless when simulating at $T = \infty$). Thus it would be beneficial to have a method which is significantly faster if a spin does not flip; reminiscent of the kinetic Monte Carlo approach [28, 29]. The kinetic Monte Carlo approach is rejection free and one chooses which spin will flip according to its proposed energy change. In succession one then updates the time according to how long this spin flip would have taken in a Metropolis Monte Carlo simulation. We, however, have taken another approach which will be explained in the context of the Ising model with the archetypical Hamiltonian of (1). In our approach, we store the effective field h_j for every spin s_j , where

$$h_j = \sum_i J(r_{i,j})s_i. \quad (7)$$

This enables us to calculate ΔE_i , the change in energy if spin s_i would flip, in a very efficient way:

$$\Delta E_i = 2s_i h_i. \quad (8)$$

Using the proposed formulation, one only would need to recalculate the h_j for all $j \neq i$ if a spin flips. However, there is a much more efficient way to do this. We can instead iterate over the lattice and update all $h_j \rightarrow h_j + 2s_i J(r_{i,j})$, making this operation comparable in speed to a single calculation of ΔE_i . For the nearest-neighbor Ising model, one would thus only update the effective field of the surrounding spins (4 in a two-dimensional, 6 in a three-dimensional simple-cubic lattice). This leads to a speedup of only $\approx 10\% - 20\%$ when simulating below the critical temperature T_c , because the computational effort of calculating $\Delta E_i = 2s_i J(1) \sum_{\langle ij \rangle} s_j$ is roughly comparable to calculating $\Delta E_i = 2s_i h_i$ (here $\langle ij \rangle$ refers to all j with $r_{ij} \equiv 1$). However, for long-range interactions this difference is very big, thus leading to significant speedups. In Ref. [25], we found a speedup of $\approx 10^3$ for the Metropolis simulation of coarsening in the two-dimensional Ising model.

2.2. Ewald summation

When dealing with long-range interactions, the finite-size effects become very strong. In this work, we chose the power-law like decaying potential presented in (2). For long-range interacting systems, one often uses periodic boundary conditions via the minimum-image convention. Another way to imitate periodic boundary conditions and to minimize the effect of a finite system size is the Ewald summation [30, 18]. The basic idea is to envision infinitely many copies or identical image systems in all directions. One then can identify the distance of each replica by $\vec{v} = (m_x, m_y)$, where $m_i = 0, \pm L, \pm 2L, \dots$ for $i = x, y$ and L is the linear size of the system. The interaction strength between two spins can then be more accurately calculated as

$$J^*(s_i, s_j) = \sum_{m_x} \sum_{m_y} \frac{1}{|\vec{v} + \vec{r}_{ij}|^{d+\sigma}}. \quad (9)$$

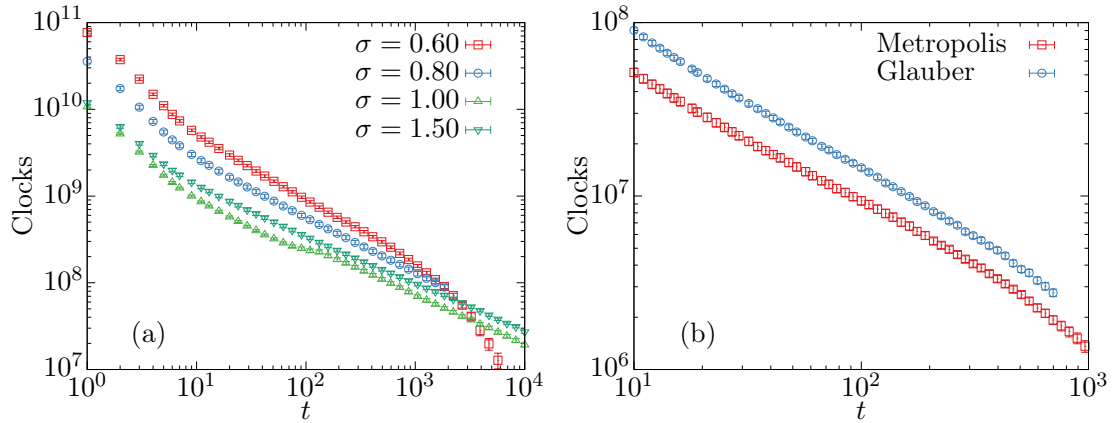


Figure 1. The number of clocks needed per sweep vs. time t for (a) different values of σ with $L = 2048$ using the Metropolis criterion and (b) for $\sigma = 0.6$ with $L = 1024$ using the Metropolis and the Glauber criterion. The system was quenched to $T = 0.1T_c$ from an initially random configuration.

However, in principle this sum has to be performed over infinitely many mirror systems due to slow convergence. Luckily, one way to significantly speedup the convergence is to split the sum in a sum in real space and a sum in reciprocal space:

$$J^* = J_s^* + J_l^*, \quad (10)$$

where J_s^* is the short-range term and J_l^* is the long-range term. Those sums can be expressed as

$$J_s^* = \sum_{\vec{v}} \frac{1}{\Gamma\left(\frac{d+\sigma}{2}\right)} \frac{1}{|\vec{v} + \vec{r}_{ij}|^{d+\sigma}} \Gamma\left(\frac{d+\sigma}{2}, (\kappa|\vec{v} + \vec{r}_{ij}|)^2\right), \quad (11)$$

$$J_l^* = \frac{2\pi^{\frac{d}{2}}}{\Gamma\left(\frac{d+\sigma}{2}\right) V} \sum_{\vec{k}} \cos(2\pi\vec{k}\vec{r}_{ij}) \frac{1}{2} (\pi k)^\sigma \Gamma\left(-\frac{\sigma}{2}, \left(\frac{\pi k}{\kappa}\right)^2\right). \quad (12)$$

Here $\Gamma(x) = \int_0^\infty t^{x-1} e^{-t} dt$ is the gamma function and $\Gamma(s, x) = \int_x^\infty t^{s-1} e^{-t} dt$ is the incomplete gamma function. Both gamma functions were evaluated numerically by the GNU scientific library (GSL). The value of κ is important for the speed of convergence and was chosen to $\kappa = 2/L$ in accordance with Ref. [18]. The approach of using Ewald summation to determine a more accurate representation of the interaction potential is widely used, e.g., in long-range interacting all-atom simulations of peptides [31]. There, the positions of the particles are not fixed and this approach is used “on-the-fly”, whereas in our simulation the positions of the spins are fixed and J^* is calculated only once at the beginning of the simulation for every pair of σ and L .

3. Results

We now want to use the above introduced methodology for simulating the coarsening in the two-dimensional Ising model with long-range interactions for different values of σ and for the mentioned acceptance criteria according to Metropolis and Glauber.

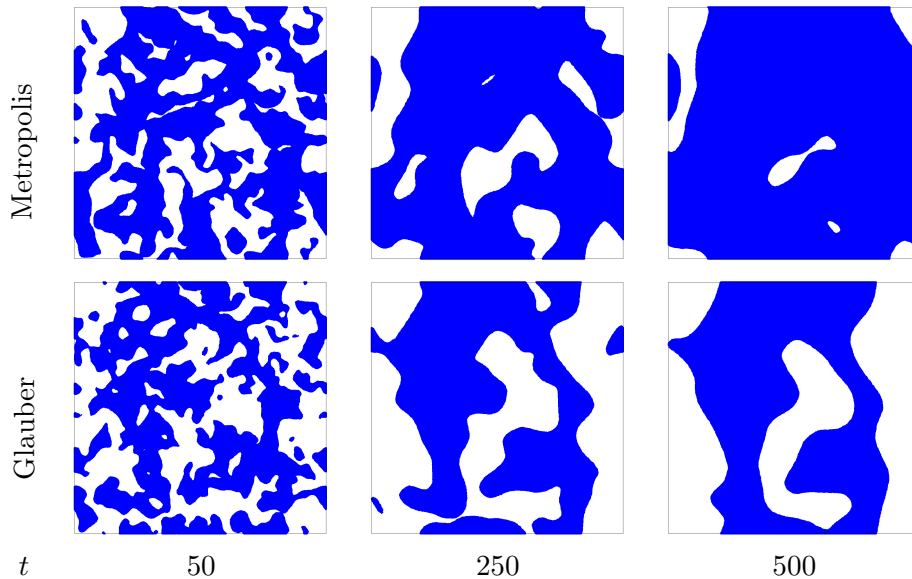


Figure 2. Snapshots at time t of the evolution for a single seed using the Metropolis (upper panels) and Glauber (lower panels) update criterion for $\sigma = 0.6$ and $L = 1024$ when the system is quenched from a random start configuration to $T = 0.1T_c$.

3.1. Runtime analysis

In Figs. 1(a) and (b) we show the dependence of the clocks needed per sweep versus the time t for (a) different σ using the Metropolis criterion and for (b) $\sigma = 0.6$ using both the Metropolis and Glauber criterion. It becomes clear from this figure, that the runtime per sweep dramatically decreases as the systems becomes more ordered, indicating that less spin-flip attempts are successful. In the scaling region, one can observe a power-law like decay with varying exponent, depending on σ . If one would not store the effective field, the number of clocks per sweep would be roughly constant for all times and always greater than the presented data. One important factor, somehow neglected in the above graph, is the additional time needed to calculate the initial h_j . In principle, this overhead could be so big, that this approach is not advantageous anymore. However, one can reformulate the algorithm in such a way, that the runtime is always strictly below the runtime of the traditional algorithm (details will be presented in Ref. [32]). The comparison presented in Fig. 1(b) shows that for $\sigma = 0.6$ and $L = 1024$, the Glauber criterion generally has a bigger number of accepted spin flips in such a quench, reflected in the higher number of clocks needed per sweep for every t . It is clear, that the approach of storing the effective field per spin and subsequently updating those values significantly decreases the amount of needed computational resources. In Ref. [25], we presented such a comparison for the Metropolis criterion and found an improvement factor of $\approx 10^3$.

3.2. Kinetics of growth

In Fig. 2 we present snapshots for the coarsening of a single run for $\sigma = 0.6$ and $L = 1024$ for both the Metropolis and Glauber criterion. The system was in this work quenched to $T = 0.1T_c$, where the values of T_c , which for the long-range Ising model depend on the decay exponent σ , were extracted by a power-law fit of the form $T_c(\sigma) = T_c(\infty) + a\sigma^b$ to the data presented in Ref. [18]. For nonequilibrium studies, knowing the exact value of $T_c(\sigma)$ is not important and this rather crude estimation is sufficient. Phenomenologically, the evolution appears to be driven in a similar way as for the short-range model by reduction of phase boundaries. However, it

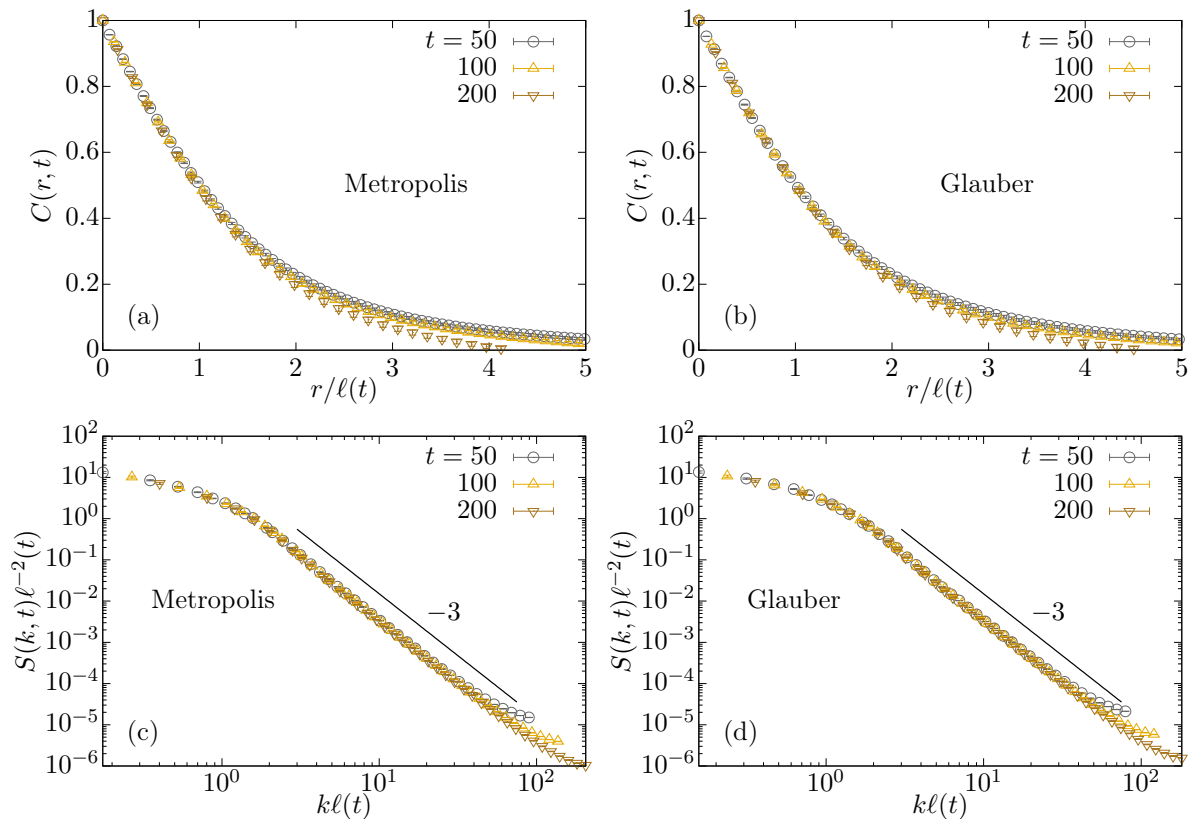


Figure 3. In (a) for the Metropolis criterion and in (b) for the Glauber criterion, the scaling of the correlation function $C(r, t)$ is shown by plotting it against $r/\ell(t)$. In (c) and (d) we present the scaling of the structure factor $S(k, t)$ for the Metropolis respectively Glauber update criterion. The solid lines with slope -3 indicate Porod's law. All presented data were obtained for systems with $\sigma = 0.6$ and $L = 1024$ with a quench temperature of $T = 0.1T_c$.

appears that the dynamics of the Metropolis update is faster than for the Glauber update, which is of course already reflected in the update criteria p_M and p_G and the analysis of the run time in Fig. 1. The starting configuration was identical for both criteria. Importantly, the phase boundaries are smooth rather than rugged.

We calculate the equal-time spin-spin correlation function

$$C(r, t) = \langle s_i s_j \rangle - \langle s_i \rangle \langle s_j \rangle \quad (13)$$

to quantify the coarsening. With increasing time after the quench, the correlation is expected to become stronger, i.e., $C(r, t)$ decays slower. From this fact, one can then extract a length scale $\ell(t)$ by taking the intersection of the correlation function with a constant value $c \in (0, 1)$. We chose $C(r, t) = \text{const.} = 0.5$ as one often does in simulations of coarsening. In Figs. 3(a) and (b) the data collapse of $C(r, t)$ if plotted against $r/\ell(t)$ for (a) the Metropolis criterion and (b) the Glauber criterion. This scaling is predicted by theory. For later times t and larger r , one sees some deviation of the collapse, which we attribute to the very strong finite-size effects. However, overall the collapse is very good. Next we analyse the scaling of the structure factor $S(\vec{k}, t) = \int d\vec{r} C(\vec{r}, t) e^{i\vec{k}\vec{r}}$, the Fourier transform of the correlation function $C(r, t)$ in Fig. 3(c) for the Metropolis criterion and in (d) for the Glauber criterion. The data collapse is very good, until at high $k\ell(t)$ the finite-size effects come into play. The decay follows a power law with

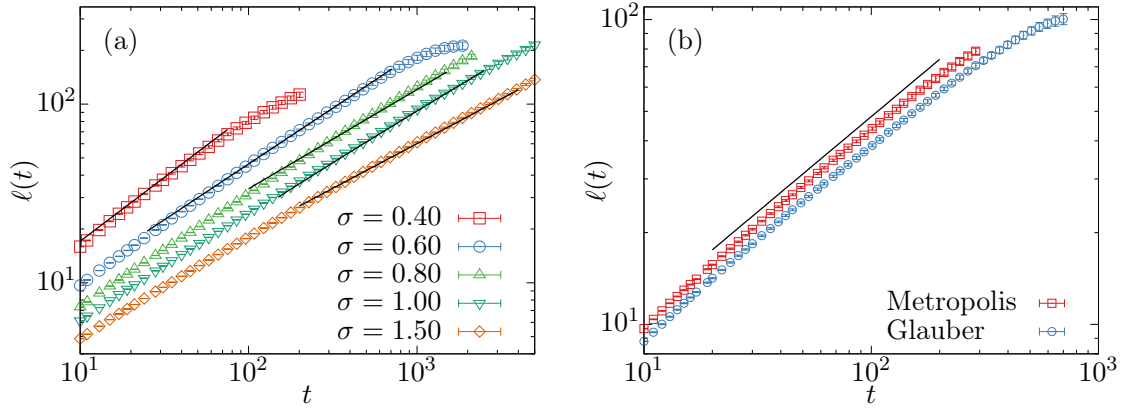


Figure 4. (a) Growth of length scale $\ell(t)$ with time t using the Metropolis update for different σ for $L = 2048$. In (b) the growth of $\ell(t)$ is shown for both the Metropolis and Glauber criterion for $\sigma = 0.6$ and $L = 1024$. The solid lines in (a) and (b) correspond to the prediction (3).

exponent -3 , in accordance with Porod's law [33]. This fact is used in the derivation of (3) and thus is important. With this necessary condition of the coarsening being a scaling phenomenon out of the way, we now aim to quantify the growth of $\ell(t)$.

To quantify the differences in the growth of $\ell(t)$ for different σ , we simulated the coarsening for $L = 2048$ and the Metropolis criterion. In Fig. 4(a), the characteristic length $\ell(t)$ for these simulations is shown. The solid lines here correspond to the prediction (3) with an appropriate prefactor to make the solid lines fall on top of the data. We now want to compare the Metropolis criterion to the Glauber criterion. For this, we present the corresponding plot in Fig. 4(b) for $\sigma = 0.6$ and $L = 1024$. As expected, both the Metropolis and Glauber simulations show agreement with the prediction (3) (given by the solid line in the same figure). However, the simulation using the Glauber criterion has a smaller amplitude and overall runs longer. This is in agreement with the higher number of clocks/spin flips per sweep observed in Fig. 1(b).

3.3. Exponent analysis

In Fig. 4 we can observe a good agreement with the prediction (3). However, it is always important to obtain some independent quantitative estimation of observables to mitigate the effect of observation bias. We therefore fit a power law of the form

$$\ell(t) = At^{\frac{1}{1+\sigma_f}} \quad (14)$$

to the growth of $\ell(t)$ for the Metropolis simulation with $\sigma = 0.6$ and $L = 2048$. When doing such fits, it is always very difficult to find proper ranges of minimal and maximal values of the independent variable. We therefore vary t and record the reduced chi-square χ_r^2 value and the values of the fit parameters A and σ_f . In Fig. 5(a) we present a heatmap plot, where t_{\min} is the lower bound of t and t_{\max} the upper bound of t . The colormap encodes the value of σ_f . All fits with $\chi_r^2 > 1.5$ and $\chi_r^2 < 0.5$ were discarded. One can observe that $\sigma_f = 1.0$, the value expected from such a quench in the short-range Ising model, is not present at all. One finds a rather big plateau around $\sigma_f = 0.6$, indicating this to be the correct value. If one moves towards higher values of t_{\min} , one of course observes an increase of σ_f due to finite-size effects. There is, however, no longer any plateau visible, a strong indication that $\sigma_f = 0.6$ is indeed the correct value, further validating the found results.

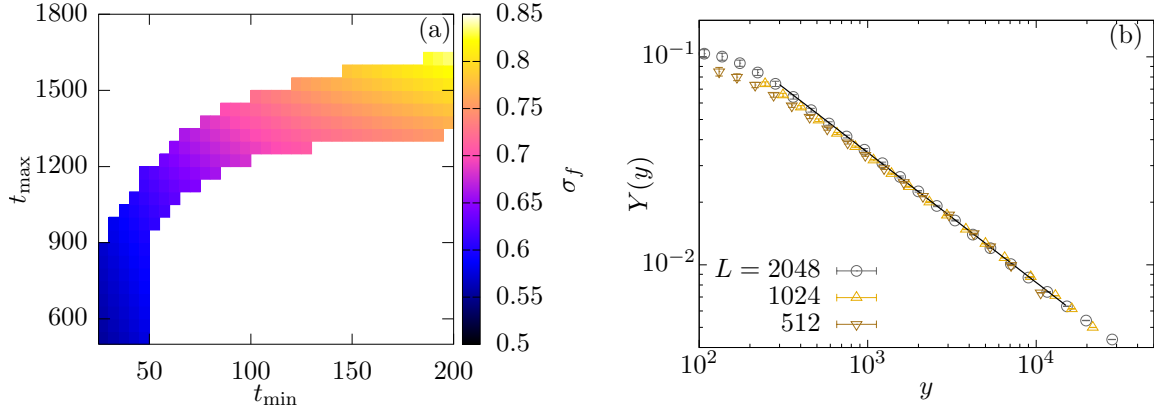


Figure 5. (a) Heatmap of the fit parameter σ_f for different ranges of the independent variable $t_{\min} \leq t \leq t_{\max}$ for a fit of $\ell(t) = At^{1/(1+\sigma_f)}$ to $\ell(t)$ for $\sigma = 0.6$ and $L = 2048$. The colormap here encodes the value of σ_f found. Only fits with $0.5 \leq \chi_r^2 \leq 1.5$ are shown. (b) Finite-size scaling analysis for $\ell(t)$ with $\sigma = 0.6$ and $L = 2048, 1024, 512$. The solid line corresponds to the predicted behavior.

To further strengthen the claim that indeed the analytic prediction is correct, we finally perform a finite-size scaling analysis [34, 35] by allowing an off-set in the asymptotic scaling law for $\ell(t)$,

$$\ell(t) = \ell_0 + At^{\frac{1}{1+\sigma}}, \quad (15)$$

where ℓ_0 is some initial length, which proved to be significant for the finite-time scaling behavior of $\ell(t)$. Then one writes down the finite-size scaling function as

$$Y(y) = \frac{\ell(t) - \ell_0}{L - \ell_0} \quad (16)$$

with appropriate choice of the argument,

$$y = \frac{(L - \ell_0)^{1+\sigma}}{t - t_0}. \quad (17)$$

In the finite-size unaffected regime, i.e., in the scaling regime it can be shown that

$$Y \sim y^{-\frac{1}{1+\sigma}}. \quad (18)$$

Thus, when plotting $Y(y)$ for different L , one expects data collapse with a slope corresponding to $y^{-\frac{1}{1+\sigma}}$. A similar analysis has previously successfully been applied in various systems [34, 35, 36, 37, 38]. In Fig. 5(b) we show such a data collapse exercise. For large values of y the data for different L collapse well and are in very good agreement with the solid line showing the power-law behavior with exponent $-1.0/1.6$ expected for $\sigma = 0.6$. For small values of y , however, one can observe a flat behavior due to the influence of finite-size effects. From the point of the deviation of the data from the asymptotic $Y \sim y^{-\frac{1}{1+\sigma}}$ behavior to the flat regime one can estimate the onset point of finite-size effects, which in our case occurs at $\ell/\ell_{\max} \approx 0.78$, where ℓ_{\max} is the maximal length scale $\ell(t)$ can attain for a finite L . Here we obtained ℓ_{\max} from the asymptotic value of $\ell(t)$ observed in Fig. 4(a). A larger value of L would manifest in a longer period of smaller values of y following the slope.

4. Conclusion

We have compared the coarsening in the two-dimensional Ising model with long-range interactions using both the Metropolis and Glauber criterion. It was confirmed that both update criteria produce results that are in agreement with the analytical prediction. We further have analyzed the runtime per sweep during a quench for both criteria. Apart from the obvious adaptation of this approach to simulate the dynamics of long-range interacting systems to other related models and the investigation of other nonequilibrium quenching properties (such as, e.g., aging or persistence [39, 32]), we would like to point out that one could also effectively investigate the Kibble-Zurek mechanism in Ising models with long-range interactions during a nonequilibrium quench [40, 41, 42, 43]. This would hopefully lead to significant new physical insight in the process of slow quenches.

Acknowledgments

This project was funded by the Deutsche Forschungsgemeinschaft (DFG) under Grant Nos. JA 483/33-1 and SFB/TRR 102 (project B04), and further supported by the Deutsch-Französische Hochschule (DFH-UFA) through the Doctoral College “ \mathbb{L}^4 ” under Grant No. CDFA-02-07, the EU Marie Curie IRSES network DIONICOS under Grant No. PIRSES-GA-2013-612707, and the Leipzig Graduate School of Natural Sciences “BuildMoNa”.

References

- [1] Lifshitz I M 1962 *J. Exp. Theor. Phys.* **15** 939
- [2] Allen S M and Cahn J W 1979 *Acta Metall.* **27** 1085
- [3] Bray A 2002 *Adv. Phys.* **51** 481
- [4] Puri S and Wadhawan V (eds) 2009 *Kinetics of Phase Transitions* (CRC Press, Boca Raton)
- [5] Bak P 1997 *How Nature Works* (Oxford University Press, Oxford)
- [6] Lux T and Marchesi M 1999 *Nature* **397** 498
- [7] Beggs J and Pleniz D 2003 *J. Neurosci.* **24** 11167
- [8] Petrs O and Neelin D 2006 *Nat. Phys.* **2** 393
- [9] Gundh J, Singh A and Singh R 2015 *PloS one* **10** e0141463
- [10] Bray A J 1993 *Phys. Rev. E* **47** 3191
- [11] Bray A and Rutenberg A 1994 *Phys. Rev. E* **49** R27
- [12] Rutenberg A and Bray A 1994 *Phys. Rev. E* **50** 1900
- [13] Stell G 1970 *Phys. Rev. B* **1** 2265
- [14] Fisher M, Ma S and Nickel B 1972 *Phys. Rev. Lett.* **29** 917
- [15] Sak J 1973 *Phys. Rev. B* **8** 281
- [16] Luijten E and Blöte H 1997 *Phys. Rev. B* **56** 8945
- [17] Luijten E and Blöte H 2002 *Phys. Rev. Lett.* **89** 025703
- [18] Horita T, Suwa H and Todo S 2017 *Phys. Rev. E* **95** 012143
- [19] Singh A, Ahmad S, Puri S and Singh S 2014 *Eur. Phys. J. E* **37** 2
- [20] Swendsen R and Wang J 1987 *Phys. Rev. Lett.* **58** 86
- [21] Luijten E and Blöte H 1995 *Int. J. Mod. Phys. C* **6** 359
- [22] Fukui K and Todo S 2009 *J. Comput. Phys.* **228** 2629
- [23] Flores-Sola E, Weigel M, Kenna R and Berche B 2017 *Eur. Phys. J. Spec. Top.* **226** 581
- [24] Hucht A, Moschel A and Usadel K 1995 *J. Magn. Magn. Mater.* **148** 32
- [25] Christiansen H, Majumder S and Janke W 2018 *preprint arXiv:1808.10426*
- [26] Metropolis N, Rosenbluth A W, Rosenbluth M N, Teller A H and Teller E 1953 *J. Chem. Phys.* **21** 1087
- [27] Glauber R J 1963 *J. Math. Phys.* **4** 294
- [28] Newman M and Barkema G 1999 *Monte Carlo Methods in Statistical Physics* (Oxford University Press, Oxford)
- [29] Voter A F 2007 *Introduction to the kinetic Monte Carlo method* in *Radiation Effects in Solids* ed Sickafus K E, Kotomin E A and Uberuaga B P (Springer, Dordrecht) pp 1–23
- [30] Ewald P 1921 *Ann. Phys.* **369** 253
- [31] Frenkel D and Smit B 2001 *Understanding Molecular Simulation: From Algorithms to Applications* (Academic Press, Cambridge)
- [32] Christiansen H, Majumder S and Janke W to be published

- [33] Porod G 1982 *General theory in Small Angle X-ray Scattering* ed Glatter O and Kratky O (Academic Press, London) p 17
- [34] Majumder S and Das S 2010 *Phys. Rev. E* **81** 050102
- [35] Das S, Roy S, Majumder S and Ahmad S 2012 *Europhys. Lett.* **97** 66006
- [36] Majumder S and Janke W 2015 *Europhys. Lett.* **110** 58001
- [37] Majumder S, Zierenberg J and Janke W 2017 *Soft Matter* **13** 1276
- [38] Christiansen H, Majumder S and Janke W 2017 *J. Chem. Phys.* **147** 094902
- [39] Henkel M and Pleimling M 2010 *Non-Equilibrium Phase Transitions, Vol. 2: Ageing and Dynamical Scaling far from Equilibrium* (Springer, Heidelberg)
- [40] Kibble T W B 1976 *J. Phys. A* **9** 1387
- [41] Zurek W H 1985 *Nature* **317** 505
- [42] Liu C W, Polkovnikov A and Sandvik A W 2014 *Phys. Rev. B* **89** 054307
- [43] Puebla R, Nigmatullin R, Mehlstäubler T E and Plenio M B 2017 *Phys. Rev. B* **95** 134104